

## Novel Tunable Optical Properties of Liquid Crystals, Conjugated Molecules and Polymers in Nanoscale Periodic Structures as Photonic Crystals

Katsumi Yoshino,\*<sup>1</sup> Hiroyuki Takeda,<sup>1</sup> Masahiro Kasano,<sup>1</sup> Shigenori Satoh,<sup>1</sup> Tatsunosuke Matsui,<sup>1</sup> Ryotaro Ozaki,<sup>1</sup> Akihiko Fujii,<sup>1</sup> Masanori Ozaki,<sup>1</sup> Akira Kose<sup>2</sup>

<sup>1</sup> Department of Electronic Engineering, Graduate School of Engineering, Osaka University, 2-1 Yamada-Oka, Suita, Osaka 565-0871, Japan

<sup>2</sup> Nihon Koken Kogyo Co. Ltd. Tachikawa, Tokyo 190-0033, Japan

**Summary:** Tunability of optical properties such as transmission and reflection by temperature and applied voltage has been demonstrated in synthetic opals and inverse opals like three-dimensional photonic crystals infiltrated with liquid crystals, conjugated molecules and polymers, in accordance with theoretical calculation. A new type of tunability based on uncoupled mode in a two-dimensional photonic band gap influenced by the field-dependent anisotropy in liquid crystals has also been demonstrated theoretically. Spectral narrowing and lasing have been observed in these opals infiltrated with conducting polymers and fluorescent dyes like three-dimensional photonic crystal and fluorescent dye-doped cholesteric and ferroelectric liquid crystal as one-dimensional photonic crystal. These lasing wavelength can be controlled by the applied voltage. Laser emission was also realized with conducting polymer on a surface relief grating formed on an azo-polymer film by interference optical beam.

**Keywords:** conducting polymer; laser, opal; liquid crystal; photonic crystal

### Introduction

Recently photonic crystals with three-dimensional periodic structures of the order of optical wavelength have attracted great interest from both fundamental and practical viewpoints because novel concepts, such as photonic band gaps in which some energy range of photons cannot exist, and also various novel applications utilizing unique characteristics of photonic crystals have been proposed.<sup>[1,2]</sup> A wide variety of applications can be realized utilizing the unique photonic band structure, i.e., utilizing photonic band gap, structure photonic band edge structure and defects in photonic crystals. Even in one-dimensional periodic structure, a photonic band gap corresponding to the stop band appears in one direction.

The photonic band gap is dependent on the refractive index, periodicity, occupation ratio, crystal structure and so on. We have proposed a tunable photonic crystal in which the photonic band structure such as band shape and band gap can be tuned by external applied

field and also by ambient conditions.<sup>[3-5]</sup> As one of the methods to realize tunable photonic crystals, various materials such as organic molecules, liquid crystals and conducting polymers can be infiltrated in interconnected nanoscale voids in synthetic opals prepared by the sedimentation of silica spheres and also in their inverse opals, which have a three-dimensional periodic structure of the order of optical wavelength and are considered as prototype photonic crystals.

In this paper, we report on the tunability and its dynamic behavior as functions of structures and materials of three-dimensional periodic structures, temperature and applied field. The results are also discussed in terms of theoretical band calculations. A new type of tunability utilizing anisotropy of liquid crystals in photonic crystals but not using photonic band gap is also discussed. Lasing characteristics are examined in opals containing organic molecules and conducting polymers like three-dimensional photonic crystals and also in cholesteric and ferroelectric liquid crystals as one-dimensional photonic crystals; their wavelength tunability is discussed. Lasing in conducting polymer in a surface relief grating formed on an azopolymer film is also discussed.

## Experimental

Synthetic opals were prepared by sedimentation of silica ( $\text{SiO}_2$ ) spheres with a diameter of several hundreds nm in water. Inverse opals were prepared by infiltrating various materials such as phenol resin in to the interconnected nanoscale periodic array of voids in the synthetic opal and subsequently removing  $\text{SiO}_2$  by a chemical treatment with HF solution. As shown in Fig.1, the inverse opals have periodic array of nanoscale voids. Various materials can be infiltrated in to these nanoscale voids of opals and inverse opals.

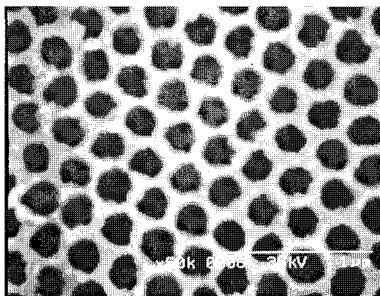


Figure 1. Scanning electron microphotograph of the inverse opal.

Polymer opals containing fluorescent dyes were also prepared by utilizing polymer (latex) nanoscale spheres doped with fluorescent dyes (Uvitex EBF (Chiba)) at 95 °C for two hours. Upon irradiation of the interference optical beam on the surface of a polymer containing azogroups in the side chain, a surface relief grating was formed. Utilizing this surface grating as a template, i.e., upon casting an other photopolymer on this surface relief of the azopolymer and then removing the surface relief, an inverse surface relief structure was formed, on which a conducting polymer film could be formed by casting chloroform solution of ROPPV (poly[(2,5-dialkoxyphenylene)vinylene]).

Cholesteric and ferroelectric liquid crystals which have helical structure are also studied as one-dimensional photonic crystals. Lasing characteristics have been studied of these liquid crystals, after doping with fluorescent dyes.

For excitation source of lasing experiment, second- or third-harmonic lights of Q-switched Nd:YAG laser (Spectra Physics, Quanta-Ray INDI) whose pulse width and pulse repetition frequency were 8 ns and 10 Hz, respectively, and a second harmonic light of a regenerative amplifier system based on a Ti:sapphire laser (Spectra Physics) whose pulse width, wavelength and pulse repetition frequency were 150 fs, 400 nm and 1 kHz, respectively, were used. The emission spectra of the sample were measured using a CCD multichannel photodetector (Hamamatsu Photonics, PMA-11) having spectral resolution of 3 nm or a spectrograph with CCD (Oriel, 256) with a 0.5 nm resolution.

## Results and discussion

### *Tunability of synthetic opals and inverse opals infiltrated with liquid crystals and conducting polymers*

Liquid crystals such as nematic liquid crystals, smectic liquid crystals including ferroelectric liquid crystals and anti-ferroelectric liquid crystals, and cholesteric liquid crystals, were successfully infiltrated in to synthetic opals made of silica spheres and their inverse opals as photonic crystals having a three-dimensional structure with a periodicity of the order of optical wavelength.

The optical stop-band in the transmission spectrum and the peak in the reflection spectrum can be tuned by temperature and also by the applied voltage in the spectral range covering from ultraviolet to infrared. A sharp peak in the reflection spectrum and a dip in the transmission spectrum observed in the synthetic opal shifted drastically upon infiltration of liquid crystals in the nanoscale voids of opals. They also shifted to shorter wavelengths upon

increasing temperature, showing a stepwise change at the phase transition point as shown in Fig. 2. These results well coincide with the theoretical analysis.

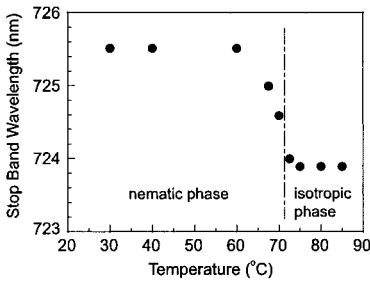


Figure 2. Temperature dependence of the peak wavelength of optical stop-band in a synthetic opal infiltrated with a nematic liquid crystal (ZLI1132, Merck).

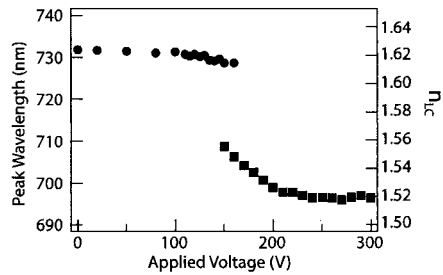


Figure 3. Voltage dependence of the peak wavelength of stop-band in the reflection spectrum of the polymer inverse opal infiltrated with 5CB.

The shifts of peaks in reflection spectra and dips in transmission spectra due to infiltration and temperature change were larger in the case of inverse opal, which can be explained by a larger volume fraction of voids in the inverse opal than in the original opal.

Upon voltage application the peak and dip in spectra also shifted to shorter wavelength as shown in Fig. 3. It should be noted that there exists a hysteresis. The tuning of the optical properties by applying a voltage above some threshold voltage has been interpreted in terms of the change of refractive index of infiltrated liquid crystals accompanied by a field-induced reorientation of liquid crystal molecules. The threshold originates from the intense interaction of liquid crystal molecules and the inner surface of the void.

The switching time, in particular the rising time upon field application was much faster than that of a conventional nematic liquid crystal cell and decreased proportionally to the square of the applied field, which suggests that the driving torque for molecular reorientation originates from dielectric force.

In the case of the inverse opal infiltrated with nematic liquid crystals, a similar change of the peak was observed but at a certain voltage the peak disappeared, which can be explained by the coincidence of the refractive index of liquid crystals to that of polymer. At higher fields, the peak again shifts to shorter wavelengths with a higher rate. This suggests that the surface anchoring force also influences dynamic characteristics.

The deformation of sphere voids in the polymer replica also has some effects on the tuning behavior.

Opals and inverse opals infiltrated with smectic liquid crystals and cholesteric liquid crystals also exhibited novel characteristics. Their dynamic behavior is determined by the origin of the driving force of the molecular reorientation of the liquid crystal due to the applied field. In the case of nematic liquid crystals, for example, the response time decreased with increasing the applied voltage proportional by to the reciprocal of the square of the applied voltage. In the case of the photonic crystal infiltrated with ferroelectric liquid crystals with spontaneous polarization  $P_s$ , the torque seems to originate in the  $P_s E$  torque.

The stop-band and reflection peak in the spectra and the dynamic behavior upon field application at various temperatures were confirmed to depend on the periodicity of photonic crystals and the material forming photonic crystal (opals and replicas).

We have theoretically studied the photonic band structure of photonic crystals infiltrated with liquid crystals and found a new type of tunability in two-dimensional photonic crystals infiltrated with anisotropic liquid crystals. We have calculated the photonic band structure of a two-dimensional photonic crystal made of liquid crystal columns in square lattice, utilizing the wave equation modified by magnetic field.

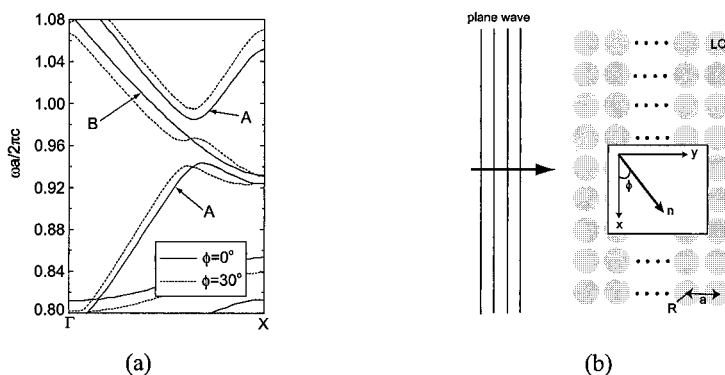


Figure 4. (a) Photonic band structures of two-dimensional photonic crystals made of liquid crystal columns as a function of liquid crystal molecular orientation  $\phi$ . A and B represent the symmetric and antisymmetric modes, respectively. (b) Schematic model of plane waves incident on photonic crystals composed of liquid crystals.  $n$  and  $\phi$  show the director and molecular orientation of liquid crystals.

By the analysis, it was clarified that the uncoupled modes in two-dimensional photonic crystals, which exist in the case of random orientation of liquid crystals, disappear when anisotropy appears due to the alignment of liquid crystal molecules upon voltage application.

The solid and dotted lines in Fig. 4a indicate the photonic band structures with anisotropic liquid crystals of orientation of  $\phi = 0^\circ$  and  $\phi = 30^\circ$ , respectively. Here,  $\phi$  is the angle between the director of liquid crystal molecules and the plane perpendicular to the optical beam as shown in Fig. 4b. For these structures, the optical transmittance when directors of liquid crystals are oriented at  $\phi = 0^\circ$  and  $\phi = 30^\circ$  are shown in Fig. 5. This result indicates that the reorientation of liquid crystal molecules by the applied field results in the transmission change. We are preparing the experiment to support this new idea.

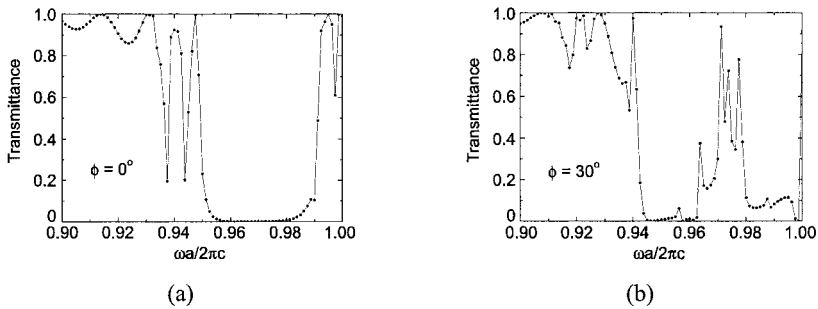


Figure 5. Transmission spectra of two-dimensional photonic crystal made of liquid crystal columns as a function of molecular orientation of the liquid crystals,  $\phi$ .

### *Spectral narrowing and lasing in opals infiltrated with conducting polymers and polymer opals containing dyes*

We have already reported observations of lasing in synthetic opals and inverse opals infiltrated with various dyes and conducting polymers. In those cases, lasing was clearly observed when fluorescence wavelengths of the dyes and conducting polymers overlap with the photonic band edge of the opals and inverse opals. For example, blue laser emission was observed in the coumarin-infiltrated opals made of 180 nm silica spheres, on the other hand, green and red laser emissions were observed when RO-PPV and cyanine dye were infiltrated into the green and red opals which were made of 220 nm and 250 nm silica spheres, respectively.

We have also studied lasing with polymer opals. Figure 6 shows the electron microscope images of the surface of plastic opals and surface of broken opals. As evident from this figure, the three-dimensional periodic structure is realized with a regular array of plastic spheres.

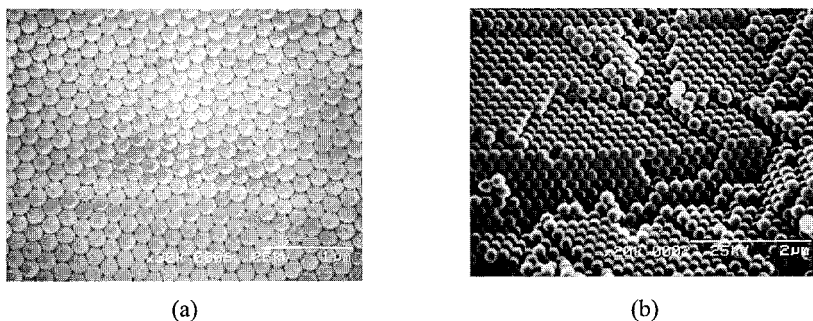


Figure 6. The scanning electron microscope images of plastic opal.

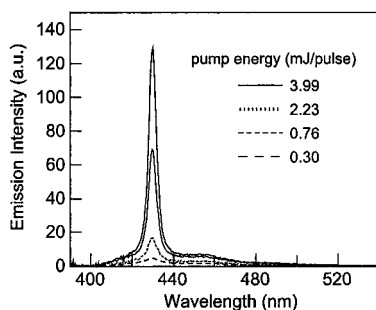


Figure 7. Emission spectra of plastic opal containing Uvitex EBF as a function of the pump energy.

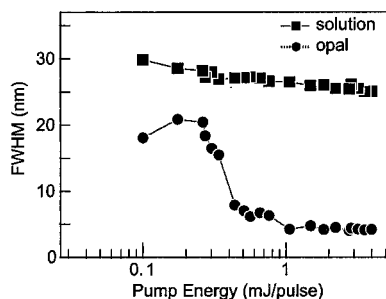


Figure 8. Emission peak width (FWHM) of plastic opal containing Uvitex EBF as a function of the pump energy.

As shown in Fig. 7, the emission intensity of opals prepared from the spheres containing Uvitex EBF increases drastically and the spectral width becomes narrower with increasing excitation intensity of THG (355 nm) of Nd-YAG laser. The spectral narrowing above some threshold excitation intensity in the dye-doped plastic opal is more clearly shown in Fig. 8. This can be explained by amplified spontaneous emission and lasing.

#### ***Surface relief grating made on azo-polymer film and lasing***

Upon irradiating the interferential light beams on the azo-polymer, the trans-cis isomerization of azobenzene in the side chain induces mass transport and forms the surface relief grating (SRG) corresponding to the distribution of the intensity of the interfered laser light. The formed SRG can be transferred onto a photopolymer using the following procedure. A sandwiched cell was fabricated using an azo-polymer film with the SRG and a glass substrate. A UV-curable prepolymer was inserted into the sandwiched cell, and cured by the UV

irradiation. After removing the substrates, a flexible polymer film with an SRG was obtained. Figure 9 shows atomic force microscope images of the holographically fabricated SRG on the azo-polymer film and the transferred inverse SRG on the photopolymer.

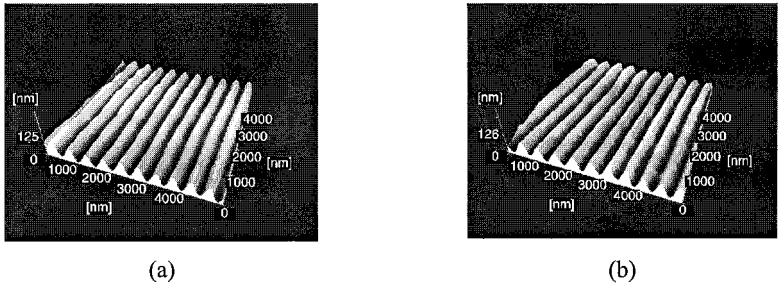


Figure 9. Scanning electron microscope images of (a) surface relief grating on azo-polymer and (b) the inverse surface relief grating on photopolymer.

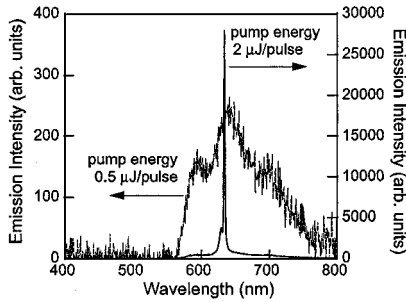


Figure 10. Emission spectra of RO-PPV coated on the inverse surface relief grating as a function of the pump energy.

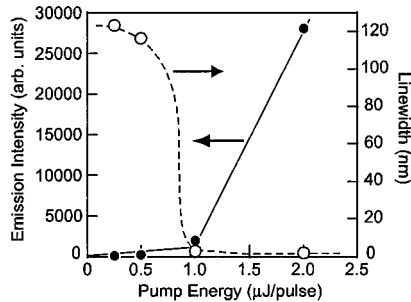


Figure 11. Pump energy dependences of emission intensity and peak width of the emission spectrum of RO-PPV on the inverse surface relief grating.

Figure 10 indicates emission spectra of RO-PPV coated on the photopolymer with the inverse SRG as a function of energy of the excitation light (532 nm). As evident from this figure, upon intense excitation a sharp emission peak was observed compared with the broad emission at low excitation intensity. Figure 11 shows the dependences of the emission intensity and spectral width on the excitation energy. As evident from this figure, above the threshold the emission intensity increases and spectral width decreases drastically. These facts clearly indicate that the mirrorless lasing was realized by the simple method. The periodicity of the inverse surface relief grating can be easily controlled by changing the incident angle of the writing interference light beam and various other light-emitting conducting polymers and



also insulating polymers containing light-emitting molecules can be overcoated on the inverse relief. Therefore, the laser device with various emission wavelength can be easily fabricated by this procedure.

***Cholesteric liquid crystal and ferroelectric liquid crystal as one-dimensional photonic crystal and lasing***

Cholesteric liquid crystals and ferroelectric smectic liquid crystals containing chiral carbon have helical structure with a pitch in the range of several hundreds of nm and several hundreds of  $\mu\text{m}$ . Therefore these liquid crystals exhibit properties of one-dimensional photonic crystals. We have incorporated fluorescent dyes in these liquid crystals and observed a laser action upon optical excitation.

Low-molecular-weight cholesteric liquid crystals (CLCs) were sandwiched between glass plates and the lasing can be observed in this sandwiched configuration. However, polymerized cholesteric liquid crystals (PCLC) can be used in a free-standing configuration without glass substrates, i.e. as flexible film.

PCLC film was fabricated utilizing two types of photopolymerizable CLC mixture (Merck KGaA). DCM as fluorescent dye was dissolved in the PCLC.

Figure 12a shows transmission spectrum of the DCM-doped PCLC. The transmittance drop at around 600 nm is due to the selective reflection corresponding to the pitch of the helix. As evident in Fig.12b, the fluorescence spectrum exhibits remarkable narrowing with increasing excitation intensity. Figure 13 shows the dependence of the emission intensity and spectral width on the excitation intensity. These figures clearly indicate that the lasing is performed in the PCLC film. It should be mentioned that the lasing can be observed in the bent film and even focusing of the laser emission was realized utilizing a spherically curved PCLC film upon optical excitation.

Laser action based on a twist defect mode was also demonstrated in a composite film composed of two dye-doped PCLC layers. The twist defect was introduced as a discontinuous jump of the director rotation around the helical axis at an interface of two PCLC layers. At high excitation energy above the threshold, the laser action was observed at the twist defect mode wavelength in the middle of 1-D photonic band gap of the PCLC helical structure.

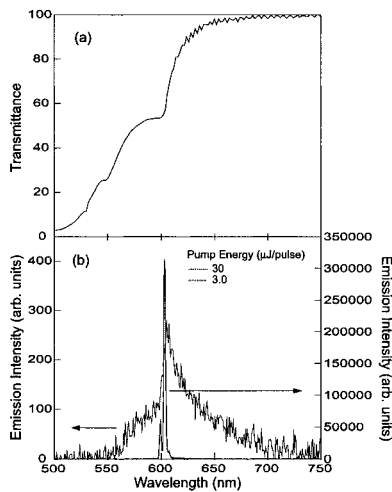


Figure 12. Transmission (a) and fluorescence (b) spectra of the DCM-doped PCLC film.

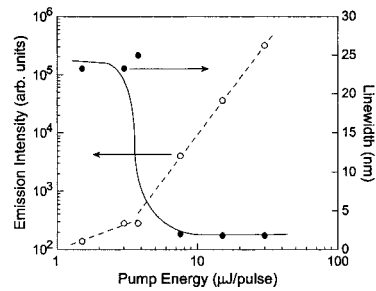


Figure 13. Pump energy dependences of emission intensity and peak width of the emission spectrum of the DCM-doped PCLC film.

Lasing was also observed in fluorescent-dye-doped ferroelectric liquid crystal (FLC). FLC mixture with a short helical pitch containing a fluorescent dye (Coumarin 500) was sandwiched between two ITO glass plates. We prepared two types of cells with different orientations, homeotropic and homogeneous cells with the helical axis parallel and perpendicular to the glass plate. In both, cases upon optical excitation, laser emission was observed in the directions parallel and perpendicular to the cell.

As evident from Fig. 14, the intensity increases and spectral width decreases with increasing excitation intensity above the threshold intensity. Lasing was observed at the edge of the photonic band gap, i.e., at the stop-band edge.

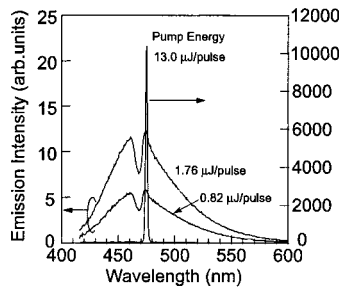


Figure 14. Emission spectra of dye-doped ferroelectric liquid crystal as a function of the pump energy.

It should be stressed that the lasing wavelength shifted drastically with increasing applied voltage as shown in Fig. 15. Therefore, the photonic band gap of the FLC was confirmed to be shifted with the applied voltage as shown in Fig. 16. This clearly supports that the voltage tunability of lasing wavelength originates from the voltage tunability of the photonic band gap.

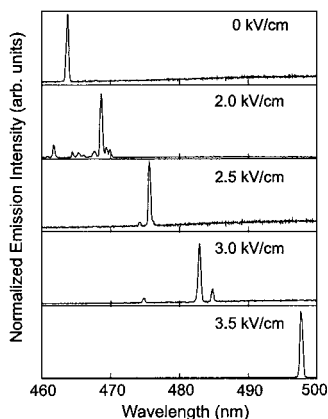


Figure 15. Lasing spectra of a dye-doped FLC as a function of applied electric field.

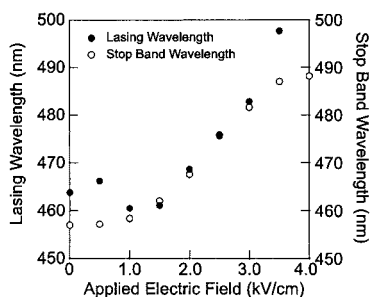


Figure 16. Electric field dependence of helix pitch and lasing wavelength of a dye-doped FLC.

## Conclusions

We demonstrated tunable optical properties of liquid crystals, conjugated molecules and polymers with nanoscale periodic structures as photonic crystal. Optical properties such as transmission and reflection were tuned by changing temperature and applying voltage to synthetic opals and inverse opals infiltrated with liquid crystals, conjugated molecules and polymers. Calculations were performed of a novel type of tunability based on uncoupled mode in a two-dimensional photonic band gap influenced by the field-dependent anisotropy in liquid crystals. Spectral narrowing was demonstrated using a plastic opal prepared from the spheres containing a fluorescent dye as three-dimensional photonic crystal. The dye-doped cholesteric and ferroelectric liquid crystals were used as one-dimensional photonic crystal, and the laser actions in these systems were demonstrated. Especially in the latter system, the lasing wavelength could be controlled by the applied voltage. Laser emission was also realized with conducting polymer on a flexible photopolymer with a surface relief grating transferred from the azo-polymer film.

## Acknowledgements

The authors would like to acknowledge Prof. F. Kajzar for providing the azo-polymer, Prof. W. Haase for the short pitch ferroelectric liquid crystal and the Merck KGaA for the photopolymerizable cholesteric liquid crystal. This work is in part supported by a grant-in-aid for scientific research from the Japan Ministry of Education, Culture and Sports, Science and Technology.

- [1] E. Yablonovitch, Phys. Rev. Lett. **58**, 2059, 1987.
- [2] S. John, Phys. Rev. Lett. **58**, 2486, 1987.
- [3] K. Yoshino, K. Tada, M. Ozaki, A. A. Zakhidov, R. H. Baughman, Jpn. J. Appl. Phys. **36**, L714, 1997.
- [4] K. Yoshino, S.B. Lee, S. Tatsuhara, Y. Kawagishi, M. Ozaki, A.A. Zakhidov, Appl. Phys. Lett. **73**, 3506, 1998.
- [5] K. Yoshino, S. Tatsuhara, Y. Kawagishi, M. Ozaki, A.A. Zakhidov, Z.V. Vardeny, Jpn. J. Appl. Phys. **37**, L1187, 1998.
- [6] K. Yoshino, S. Tatsuhara, Y. Kawagishi, M. Ozaki, A.A. Zakhidov, Z.V. Vardeny, Appl. Phys. Lett. **74**, 2590, 1999.
- [7] S. Sato, H. Kajii, Y. Kawagishi, A. Fujii, M. Ozaki, K. Yoshino, Jpn. J. Appl. Phys. **38**, L1475, 1999.
- [8] K. Yoshino, S. Satoh, Y. Shimoda, Y. Kawagishi, K. Nakayama, M. Ozaki, Jpn. J. Appl. Phys. **38**, L961, 1999.
- [9] K. Yoshino, Y. Shimoda, Y. Kawagishi, K. Nakayama, M. Ozaki, Appl. Phys. Lett. **75**, 932, 1999.
- [10] K. Yoshino, Y. Kawagishi, M. Ozaki, A. Kose, Jpn. J. Appl. Phys. **38**, L784, 1999.
- [11] Y. Shimoda, M. Ozaki, K. Yoshino, Appl. Phys. Lett. **79**, 3627, 2001.
- [12] M. Ozaki, Y. Shimoda, M. Kasano, K. Yoshino, Advanced Materials **14**, 514, 2002.
- [13] T. Matsui, R. Ozaki, K. Funamoto, M. Ozaki, K. Yoshino, Appl. Phys. Lett. **81**, 3741, 2002.
- [14] M. Ozaki, M. Kasano, D. Ganzke, W. Haase, K. Yoshino, Advanced Materials **14**, 306, 2002.
- [15] T. Matsui, M. Ozaki, K. Yoshino, F. Kajzar, Jpn. J. Appl. Phys. **41**, L1386, 2002.